

Experimental Study of Early-Stage Dynamics of the Ascending and Descending Laminar Hydrogen-Air Flames in Vertical Closed Rectangular Tube

N.B. Anikin, A.A. Tyaktev, I.A. Kirillov*, V.A. Simonenko

Federal State Unitary Enterprise “Russian Federal Nuclear Center - Zababakhin All-Russia Research Institute of Technical Physics”

Snezhinsk, Chelyabinsk region, Russia

*National Research Center “Kurchatov Institute”,

Moscow, Russia

1 Introduction

Hazard of flames is tightly related with their morphology. Up to this moment, dynamics and morphology of the flames with pronounced baric effects have been comprehensively studied, in first turn, the laminar deflagrations (cellular and pulsating), turbulent accelerated (tulip-like, finger-like, and choked) flames and detonation waves in lean, rich and near stoichiometric hydrogen-air mixtures. Previous experimental studies of the quasi-isobaric flames were centered, mainly, on their visualization without attempts to establish a unified classification and quantitative characterization of the ultra-lean combustion. The upward free ultra-lean hydrogen-air flames were studied in a vertical rectangular tube using high fidelity schlieren video system under normal temperature and pressure at MUT facility.

In order to close a gap in the ultra-lean flame classification a systematic recording of the complete changes of combustion appearance in response to gradual changes in mixture stoichiometry (from 4 to 16 vol.% H₂, with an increment down to 0.2 vol.% H₂ nearby some equivalence ratios) was made. Three basic morphological patterns of the ultra-lean quasi-isobaric hydrogen-air combustion – “raspberry-like”, “vortex-like”, “cellular (or wrinkled)”, and one transient pattern – “mushroom-like” – have been delineated. Each of the detected flame morphotype exists and is stably reproduced within the appropriate concentration limits. Received experimental databases can be used for validation of the CFD models for ultra-lean combustion, development of the new methods to study kinetics and refining the rules and criteria of lower explosive limit in hydrogen-air mixtures.

2 Experiment

The morphotypes of flames in homogeneous hydrogen-air mixtures were studied in a shortened (950 mm) part of a multi-function shock tube (MUT) of the square section of 138×138 mm². The experimental setup is presented in Figure 1.

The gas mixtures were pre-mixed in 10 l gas cylinders at the total pressure of 4 atm. The mixture compositions were controlled by partial pressures. The mixture composition error was determined by

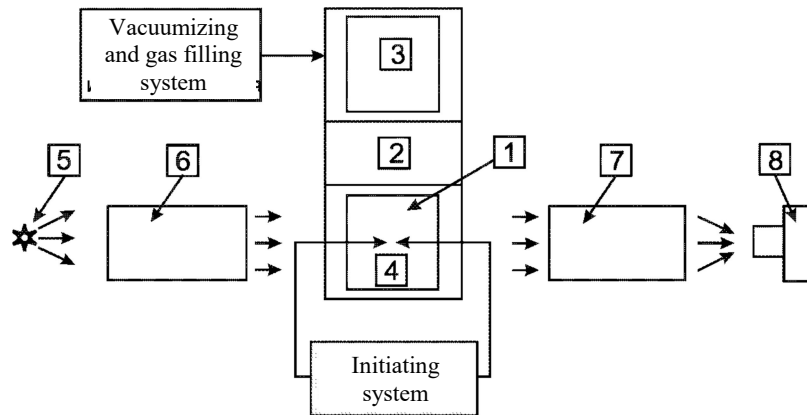


Figure 1 – Experimental setup with MUT facility. 1, 3 – measurement sections; 2 – intermediate section; 4 – initiating spark gap; 5 – light source; 6 – lighting part of IAB-451 shadow instrument; 7 – receiving part of IAB-451 shadow instrument; and 8 – high-speed digital video camera.

manometer accuracy and did not exceed 0.2 vol. %.

The evolution of flames was studied in a hermetically sealed shock tube setup.

Directly before the experiment, the shock tube was filled with a pre-mixture. The experiments started with flame initiation by a high-voltage discharge in a spark gap located at the distance of 145 mm from the bottom flange of the tube. The spark gap was formed by two tungsten electrodes 1 mm in diameter. Single high-voltage pulse igniting the mixture was generated at the pulse amplitude of 16 kV and duration of 10 μ s. Measurements were synchronized with the igniting pulse.

In each experiment, the energy released in the spark was measured, its magnitude being determined by the spark gap length (usually 1.5-3 mm) and the ballast resistor connected in series with the gap within the loading circuit of the high-voltage generator. In the experiments with the mixtures 6-16 vol.% H₂, the measured energy release was varied at a random manner within the range of 1 \div 11 mJ.

In ultra-lean mixtures (4 \div 5 vol.% H₂), more energy was required for the ignition; thus, a larger gap (7 mm) and a smaller ballast resistor were used; at that, the measured energy contribution was 66 \div 166 mJ.

The pressure dynamic within the tube was measured using D5007G pressure gauge.

The flame evolution was investigated in the measurement section (item 1 in Figure 1) of the shock tube through high-rate shadow (schlieren) video recording using IAB-451 shadowgraph and a high-speed video camera (item 8 in Figure 1). The shadow pictures of 134 \times 201 mm² format were obtained. An ultra-bright green LED Luminus CBT 120G was applied as a light source in continuous mode. Shadow pictures were used to plot X-t diagrams that are the locations of the highest and the lowest points of the flame versus time.

3 Flame morphologies in 4 \div 16 vol.% H₂ air mixtures

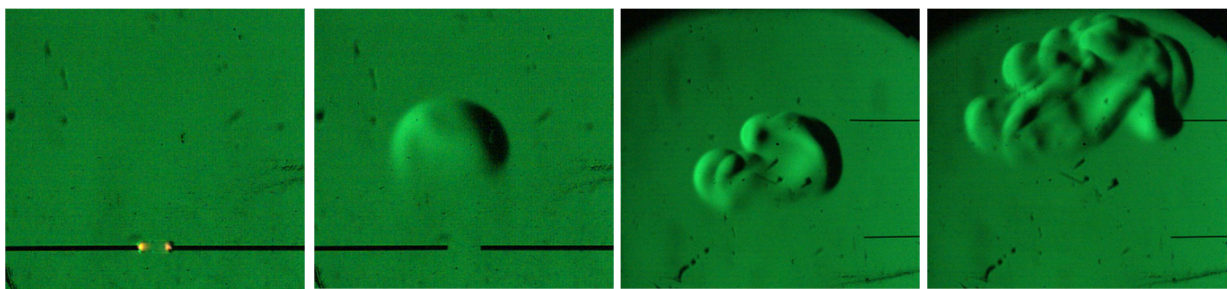
In the experiments, all the flames with H₂ concentrations of 4 \div 5 vol.% were ignited, however, for H₂ concentrations below 4.3 vol.%, they went out very fast, without losing contact with the spark electrodes. For higher H₂ concentrations, the flames once separated from the spark gap steadily

evolved. Thus, the measured concentration limit for flames upward propagation was $(4.3+4.2)/2 = 4.25$ vol.%, the error being equal to the mixture preparation error of 0.2 vol.%.

Within the whole H_2 concentration range of $4.3 \div 5$ vol.%, apparent flame velocity was about ≈ 25 cm/s and almost did not depend on the mixture composition. Clear, that the rate was determined mainly by the emersion of the flame center under the effect of buoyancy force within the Earth's gravity field.

To the moment of time $t = 37 \mu s$, the gas discharge plasma is likely to be almost decayed, and the shadow instrument records a heated and already expanded spark channel. The irradiation near the electrodes is the discharge afterglow.

The subsequent flame evolution is shown in Figures 2b-d. Starting upon time $t \approx 160$ ms when the flame reaches the typical size of ≈ 25 mm, the top surface of the flame center begins to deform and further splits into parties with a typical size of ~ 20 mm. The instability of the flame top side is



a) at time $\tau=37 \mu s$ b) at time $162 \text{ ms}+\tau$ c) at time $378\text{ms}+\tau$ d) at time $524\text{ms}+\tau$

Figure 2 – Flame in the mixture 4.5 vol% H_2 in air at different times. Picture sizes are $64 \times 60 \text{ mm}^2$ and $128 \times 120 \text{ mm}^2$ for pictures 2a, 2b and 2c, 2d, correspondingly.

explained by high sensitivity of the burning rate to flame “stretching” within the given concentration range. Note, that upon separating from the electrodes, the flame loses contrast in its bottom part. Obviously, the flame goes out on its bottom side, and keeps on propagating with the flame center “open from the bottom”.

The flames in the mixtures with H_2 concentrations below 4.3 vol.% burn up, but go out through heat dissipation to the electrodes. Steady flame «ball» size within hydrogen concentration range of $4 \div 5$ vol.% does not exceed 20 mm. Flame with a typical size over 20 mm is split into smaller «balls» forming a flame morphotype that we marked out as a “raspberry-like” one which is presented in Figures 2c through 2d.

The burning rate of the “stretched” hydrogen flame grows significantly with the decrease in concentration [1], that is why, within H_2 concentration range of $4 \div 5$ vol.%, small flame cells grow much faster than larger ones (> 20 mm) whose surfaces exhibit the development of small-scale instabilities within the Earth's gravity field.

Flames propagation in the mixtures with hydrogen concentration below 9 vol.% is controlled by the buoyancy [2]. The evolution of the “buoyant” flames begins in a similar way for all concentrations: the flame expands and simultaneously buoys upwards from the spark gap.

Flames rates within the concentration range of $6 \div 8.8$ vol.% are not high, and their evolution is essentially conditioned by the synergetic effect of the Rayleigh-Taylor instability within the Earth's gravity field and flame “stretching”. The burning rate of a non-planar flame is described by the following formula [1]:

$$S_U = S_U^0 - L_M K \quad (1)$$

where S_U^0 is the planar flame velocity, L_M is the Markstein length, and K is the Karlovitz strain factor which is defined, in turn, by the formula:

$$K = \frac{1}{A} \frac{dA}{dt},$$

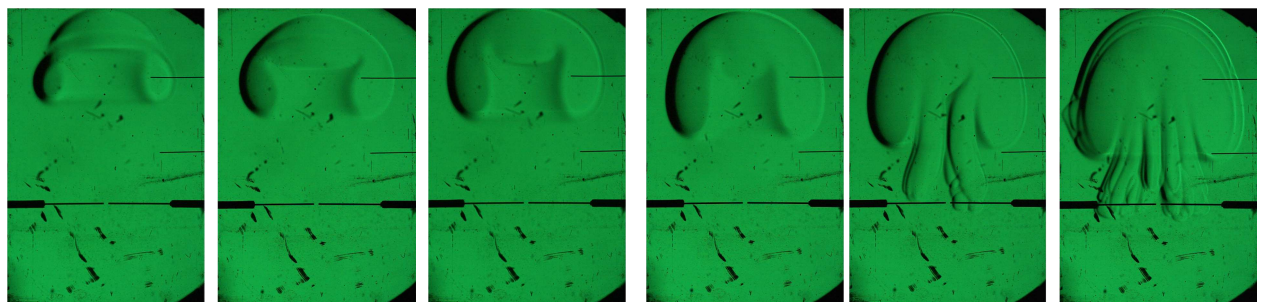
where A is the flame area.

Hydrogen flame in lean mixtures is characterized by negative and high in modulus Markstein length [1] that is why a “stretched” hydrogen flame in a lean mixture burns much faster than a planar one, and all the more “compressed” one. This feature is likely explained by selective hydrogen diffusion.

The flame, due to a high expansion coefficient of the gas mixture in flame, is subject to the Rayleigh-Taylor instability which contributes to the curvature of the flame top surface by stretching it and, thus, by accelerating the combustion on this surface. In turn, the accelerated combustion leads to the increase in temperature of the reacted mixture, and, hence, increases the density drop over the flame surface, thus, enhances the flame curvature under the Rayleigh-Taylor instability. Consequently, combustion on the flame bottom surface is characterized by positive feedback due to the Rayleigh-Taylor instability within the Earth’s gravity field. The effect of such feedback becomes weaker with the growth of the flame «ball». Note, that for the mixtures $6 \div 8.8$ vol.% H_2 within the scale below 138 mm, the top surface of the flame cell is not predisposed to splitting which is typical for leaner mixtures.

On the contrary, the bottom flame surface within the Earth’s gravity field is stable, and due to that it smooths out with time; the flame is “compressed”, therefore, according to formula (1), the combustion on the bottom surface of the flame center is decelerated resulting in a more intensive “compression” of this. Note, that “compression” of the flame center for H_2 concentrations of $4 \div 5$ vol.% leads to the extinction of the flame on its bottom surface that is unlikely to occur in the mixtures with H_2 concentrations over 6 vol.%.

Figure 3 clearly demonstrates the processes of flame cooling-down and “compression” from the bottom. The bottom surface is “indented” inwards the flame center with time. The contrast for the picture showing the bottom flame surface is weaker which bears evidence of temperature difference.



a) 6 vol.% H_2 $t=385$ ms b) 7 vol.% H_2 $t=325$ ms c) 7.5 vol.% H_2 $t=300$ ms d) 8 vol.% H_2 $t=280$ ms e) 8.6 vol.% H_2 $t=250$ ms f) 8.8 vol.% H_2 $t=235$ ms

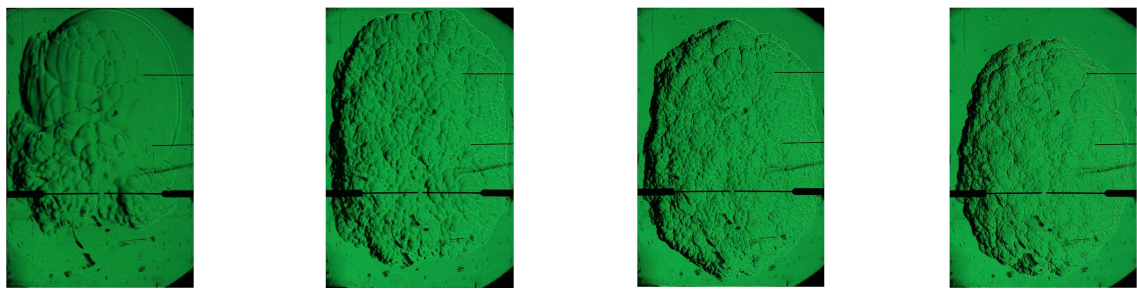
Figure 3 – “Vortex-like” flames near the upper edge of the optical window in the experiments with different H_2 concentrations. Picture size is 134×200 mm².

The above processes lead to the emergence and growth, with the upward rise, of toroidal vortex connected to the flame center. We determined the morphology of such flame as “vortex-like”. The vorticity continuously grows up under the effect of the Earth’s gravity field. Obviously, sooner or later the vortex ruptures the flame at the place where it is the most “compressed” and where the combustion is the less intensive. In Figure 3, it is clear that the flame rupture occurs in a horizontal plane. The top

part, the “cap” is pulled out and gone with the flow. Figure 3 shows the rupture in flame center for the mixture 6 % H₂. For the mixture 7 % H₂, such a rupture is just taking shape.

Despite almost two-fold growth of the flame rate within H₂ concentration range of 6 ÷ 8.8 vol.%, the evolution of “vortex-like” flames occurs similarly. We referred flame morphology within H₂ concentration range of 8.6÷8.8 vol.% to a “mushroom-like” one, being transient between “vortex-like” and “cellular” morphotypes.

In our experiment, ignition takes place in the bottom part of the tube that is why the flame is almost not restricted from the top, and, for H₂ concentrations below 8.6 vol.%, practically does not propagate downwards. However, for H₂ concentrations within 8.6 – 8.8 vol.%, the flame “catches” on massive cold electrodes and remains viable near them for a long time. A part of the flame remains just near the electrodes which cool the flame down and reduce the buoyancy force. Apparently, this part of the flame exists in a diffusion regime “collecting” the hydrogen from the bottom part of the tube while the

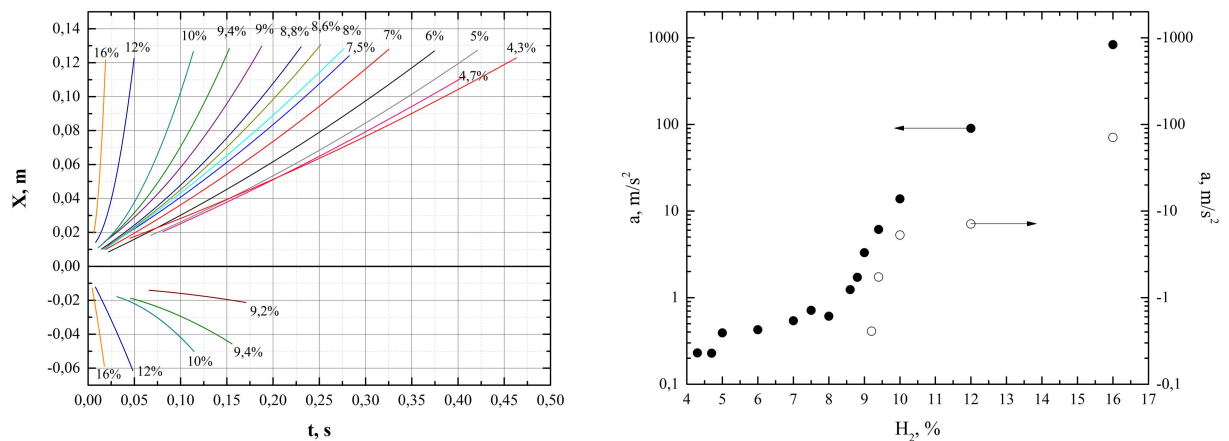


a) 9 vol% H₂, $t=190 \mu s$ d) 10 vol% H₂, $t=115 \mu s$ e) 12 vol% H₂, $t=50 \mu s$ f) 16 vol% H₂, $t=18,2 \mu s$

Figure 4 – “Cellular” flame in the mixtures with different H₂ content. Picture size is 133 × 199 mm².
main part of the flame keeps on buoying.

Further increase in H₂ concentration results in a qualitative change of flame properties that is reflected in flame transition to a “cellular” (or “wrinkled”) morphotype. At H₂ concentration of 9 vol% in air, the flame begins to propagate downwards which is demonstrated in Figure 4 where all flames are shown at the times when that they fill the field of view of IAB-451 instrument to a maximum extent.

Figure 5 plots $X-t$ diagrams and accelerations for both top and bottom surfaces of all investigated flames. All these flames are strongly shifted upwards. For H₂ concentrations below 12%, such flame behavior is explained by the effect of the buoyancy force. However, for concentrations of 12% and higher, the explanation should be different: the flame asymmetry is essentially determined by the effect of the bottom wall which restricts the flame downward propagation – the expansion of the flame center through gas heating inside it is attended with its shift upwards. The flame center expands “resting” on the bottom wall.



a) b)

Figure 5 – X-t diagrams (a) and acceleration (b) for both upward and downward parts of flames in 4-16 vol % of H₂ mixtures with air.

Note, that evolution of all flames within concentration range of 9 ÷ 16% begins from a spherical flame center which is eventually covered with a net of cells that keep on splitting. Figure 4 demonstrates the decrease in flame cell size with the change in concentration from 9 up to 16 vol.%.

Formation of the cells on the surface of the spherical flame center is explained by the effect of Rayleigh-Taylor instability which leads to self-turbulization of flames, according to [3]. Indeed, the pressure inside the flame center is always more elevated than outside, and the density inside it is always lower, that is why the surface of the expanding flame ensures the conditions favorable for instability development.

4 Conclusion

Flames in the mixtures leaner than 4.3 vol% are ignited but they do not have time to buoy and go out due to heat dissipation to the electrodes. Stable flame center size within hydrogen concentration range of 4 ÷ 5 vol.% does not exceed 20 mm. In the case of larger sizes of the flame center, small-scale instability develops within the Earth's gravity field forming a "raspberry-like" flame morphology.

Despite the almost two-fold growth of visible speed within H₂ concentration range of 6 ÷ 8.8 vol.%, flame evolution is determined by the buoyancy and the growth of toroidal vortex connected to the flame center. Such flame morphology is identified as "vortex-like".

For H₂ concentration range of 9 ÷ 16 vol.% in air, flame evolution starts with a spherical center eventually covered with a net of splitting cells. Such flame morphology is commonly named "cellular". For this concentration range, the flame propagates not only upwards, but also downwards, though asymmetrically.

For the mixtures with concentrations of 8.6% and 8.8%, "tentacles" were observed, i.e. a part of the flame remained near the electrodes which cooled the flame down and reduced the buoyancy force leaving this part of the flame in the bottom. We identified such flame morphology as "mushroom-like", which is transient one between "vortex-like" and "cellular" morphologies.

References

- [1] Gel'fand BE, Sil'nikov MV, Medvedev SP, Khomik SV. (2009) Thermal gas-dynamics of hydrogen combustion and explosion [*in Russian*]. Saint-Petersburg: Publishing of Polytechnic Institute.
- [2] Ronney PD. "Premixed-Gas Flames" in: Microgravity Combustion: Fires in Free Fall. (H. Ross, Ed.). (2001) Academic Press, London, UK. 35-82.
- [3] Gostintsev YuA, Istratov AG, Kidin NI, Fortov VE. Self-turbulization of gas flames. Theoretical interpretations [*in Russian*] High Temperature. (1999). 37, issue 4: 633-637.